Calculating surface ocean pCO_2 from biogeochemical Argo floats equipped with pH: an uncertainty analysis

N. L. Williams[1*], L. W. Juranek[1], R. A. Feely[2], K. S. Johnson[3], J. L. Sarmiento[4], L. D. Talley[5], A. G. Dickson[5], A. R. Gray[4], R. Wanninkhof[6], J. L. Russell[7], S. C. Riser[8], and Y. Takeshita[3]

[1]College of Earth, Ocean, and Atmospheric Sciences, Oregon State University, Corvallis, Oregon, USA
[2]Pacific Marine Environmental Laboratory, National Oceanic and Atmospheric Administration, Seattle, Washington, USA
[3]Monterey Bay Aquarium Research Institute, Moss Landing, California, USA
[4]Program in Atmospheric and Oceanic Sciences, Princeton University, Princeton, New Jersey, USA
[5]Scripps Institution of Oceanography, University of California San Diego, La Jolla, California, USA
[6]Atlantic Oceanographic and Meteorological Laboratory, National Oceanic and Atmospheric Administration, Miami, Florida, USA
[7]Department of Geosciences, University of Arizona, Tucson, Arizona, USA
[8]School of Oceanography, University of Washington, Seattle, Washington, USA

*Corresponding author: Nancy L. Williams (nancy.williams@oregonstate.edu)

Key Points

- Surface ocean partial pressure of carbon dioxide (pCO_{2sw}) is calculated from pH on biogeochemical profiling floats
- The relative standard uncertainty in float pCO_{2sw} estimates is 2.4% (or 10 µatm at pCO_{2sw} of 400 µatm)
- For the first time extensive wintertime pCO_{2sw} values are obtained in the Southern Ocean showing higher values than previous estimates

Abstract

More than 74 biogeochemical profiling floats that measure water column pH, oxygen, nitrate, fluorescence, and backscattering at 10-day intervals have been deployed throughout the Southern Ocean. Calculating the surface ocean partial pressure of carbon dioxide (pCO_{2sw}) from float pH has uncertainty contributions from the pH sensor, the alkalinity estimate, and carbonate system equilibrium constants, resulting in a relative standard uncertainty in pCO_{2sw} of 2.4% (or 10 µatm at pCO_{2sw} of 400 µatm). The calculated pCO_{2sw} from several floats spanning a range of oceanographic regimes are compared to existing climatologies. In some locations, such as the Subantarctic zone, the float data closely match the climatologies, but in the Polar Antarctic Zone significantly higher pCO_{2sw} are calculated in the wintertime implying a greater air-sea CO_2 efflux estimate. Our results based on four representative floats suggest that despite their uncertainty relative to direct measurements the float data can be

This article has been accepted for publication and undergone full peer review but has not been through the copyediting, typesetting, pagination and proofreading process which may lead to differences between this version and the Version of Record. Please cite this article as doi: 10.1002/2016GB005541

used to improve estimates for air-sea carbon flux, as well as to increase knowledge of spatial, seasonal, and interannual variability in this flux.

1. Background

As anthropogenic carbon dioxide (CO_2) from fossil fuel burning and land-use changes continues to build up in our atmosphere, the ocean has mediated the atmospheric increase by absorbing about 26% of emissions over the timeframe 2006-2015 [*Le Quéré et al.*, 2016]. This oceanic sink for anthropogenic CO_2 is not equally distributed throughout the world oceans but is strongest in areas of deep and intermediate water formation such as the North Atlantic and the Southern Ocean, with the Southern Ocean accounting for around half of the total oceanic uptake [*Frölicher et al.*, 2015]. Understanding how this anthropogenic CO_2 uptake occurs against the background of natural carbon fluxes is critical for understanding modern ocean changes as well as for improving climate modeling and projection.

The ocean takes up or releases CO_2 when there is a difference between the surface ocean partial pressure of CO_2 (pCO_{2sw}) and the atmospheric partial pressure of CO_2 (pCO_{2a}). The flux (F_{CO2}) of carbon between the atmosphere and the ocean can be estimated using the following bulk formula:

$$F_{CO2} = kK_0(pCO_{2sw} - pCO_{2a}) \quad (1)$$

where k is the gas transfer velocity (typically expressed as a function of wind speed) and K_0 is the solubility of CO_2 in seawater as a function of seawater temperature (T) and salinity (S). Because the atmosphere is zonally well mixed, the pCO_{2a} at any point over the Southern Ocean is nearly equal to the atmospheric CO_2 measured at a land-based observatory such as the Cape Grim Station (available from http://www.csiro.au/greenhouse-gases) for the Southern Hemisphere, corrected for local sea level pressure and the vapor pressure of water as a function of surface ocean T and S. Historically, for purposes of determining air-sea CO_2 fluxes the pCO_{2sw} is measured directly along with T and S using shipboard underway systems or moored systems. These underway and moored $pCO2_{sw}$ measurements have been favored, as no other truly autonomous systems exist. Moreover, direct pCO_{2sw} measurements at in situ T have been deemed more accurate for assessment of air-sea flux than either the discrete bottle pCO_{2sw} sampling method, in which samples are warmed to laboratory temperature before processing, or calculating pCO_{2sw} with a carbonate system calculator such as CO2SYS [*Lewis and Wallace*, 1998; *van Heuven et al.*, 2011] using discrete measurements of any two of the other carbonate system parameters [total alkalinity (TA), pH, or dissolved inorganic carbon (DIC)].

The seasonality and interannual variability in F_{CO2} is not well understood in the Southern Ocean owing to sparse observations, particularly in the austral winter. This lack of observations limits efforts to quantify annual fluxes, as well as estimates of how F_{CO2} might change in the future. There have been several community efforts to compile high-quality measurements of pCO_{2sw} and to date these compilations have been limited to direct measurements from drifter, shipboard, or moored systems. The most recent effort, the Surface Ocean CO_2 Atlas; version 4 [SOCATv4; *Bakker et al.*, 2016], includes 18.5 million fCO_{2sw} (pCO_{2sw} corrected for the non-ideal behavior of CO_2) values globally covering the years 1957−2015. Despite the large number of observations the dataset is spatially, temporally, and seasonally biased, especially in the Southern Ocean. Spatial biases arise because most Southern Ocean voyages are reoccupations of supply routes to Antarctic bases or of repeat hydrographic lines leaving large swaths of the Southern Ocean completely

unsampled (Figure 1a). Seasonal biases occur because the Southern Ocean is difficult to access especially during austral winter when dangerous weather systems are frequent, and when sea ice and icebergs may extend as far north as 50°S latitude. When comparing the distribution of SOCATv4 data from only austral winter (June-August; Figure 1b) with all Southern Ocean observations (Figure 1a) this seasonal bias becomes apparent.

From such data compilations researchers have developed data products for surface ocean pCO_{2sw} and for F_{CO2} such as the global monthly climatologies presented by *Takahashi et al.* [2009, 2014] and the global monthly gridded data product presented by *Landschützer et al.* [2014, 2015]. *Takahashi et al.* [2014] used this pCO_{2sw} climatology combined with estimates of alkalinity to develop global monthly surface climatologies for pH, DIC, and the saturation states of aragonite and calcite. Efforts are taken to minimize the effects that spatial and temporal biases in the data have on these climatologies, but in much of the Southern Ocean the variability is large, the data is sparse, and such biases are unavoidable.

The Southern Ocean Carbon and Climate Observations and Modeling (SOCCOM) project (http://soccom.princeton.edu) aims to fill these observational gaps by deploying approximately 200 biogeochemical profiling floats over five years. Now in year three, the project has deployed more than 74 floats (Figure 1c). These floats are different from traditional Argo floats in that many include ice-avoidance software and all carry some combination of additional biogeochemical sensors (pH, nitrate, oxygen, fluorescence, and backscattering). The measurement of pH is of special significance; when well calibrated, this can allow the calculation of pCO_{2sw} to high precision using existing algorithms for total alkalinity (TA) that are based on other float-measured parameters (T, S, pressure [P], and O_2) [e.g., *Carter et al.*, 2016]. With current measurement accuracies the uncertainty of calculating pCO_{2sw} from TA and pH is significantly smaller than calculating it from TA and DIC [*Dickson and Riley*, 1978]. The focus of this manuscript is to assess the uncertainties that result when these profiling float data are used to calculate pCO_{2sw}.

2. Methods

To calculate pCO_{2sw} from SOCCOM biogeochemical floats, the in situ pH measured using a Deep-sea DuraFET pH sensor [*Johnson et al.*, 2016] is combined with an algorithm-based estimate for TA. The CO2SYS MATLAB program [*van Heuven et al.*, 2011; available from http://cdiac.ornl.gov/ftp/co2sys], the equilibrium constants of *Lueker et al.* [2000], *Dickson* [1990], and *Perez and Fraga* [1987], and the boron to salinity ratio of *Lee et al.* [2010] as recommended by A. Dickson [*Wanninkhof et al.*, 2016a] were used for this analysis and pH is in situ on the total hydrogen ion concentration scale. For the remainder of this manuscript the notation X (Y, Z) is used to indicate that carbonate system parameter X was calculated using CO2SYS with inputs of Y and Z.

The SOCCOM float pH sensor data are adjusted in near-real time using an empirical algorithm for in situ pH based on T, S, P, and O_2 [*Williams et al.*, 2016]. The following steps describe the pH sensor calibration adjustment process:

1) Convert shipboard bottle pH (T = 25°C and P = 0 dbar) to in situ pH (CTD T and P).
2) Determine multiple linear regression (MLR) algorithm [*Williams et al.*, 2016] to estimate in situ pH as a function of T, S, P, and O_2 using in situ pH from depths between 1000−2000 m determined from recent shipboard bottle measurements (2011 to present) from Southern Ocean and SOCCOM deployment cruises.

3) Apply MLR algorithm to float-measured T, S, P, and O_2 to obtain MLR in situ pH estimate.
4) Adjust Deep-sea DuraFET pH sensor reference potential [*Johnson et al.*, 2016] to match 1500 m sensor in situ pH to MLR in situ pH estimate using either a one-time offset correction or a time-dependent drift correction (units of yr^{-1}).
5) Apply new calibration to entire float profile.

A minimum number of adjustments are made to keep the float pH within 0.005 of the MLR algorithm estimate; the method is described in more detail by *Johnson et al.* [2016], *Wanninkhof et al.* [2016a], and *Williams et al.* [2016]. When appropriate, time-dependent drift corrections are applied to decrease bias in the pH measurements as the sensor drifts over time. Table 1 outlines the adjustments that have been made to the four SOCCOM float pH sensors utilized in the discussion. Offset adjustments are additive and cumulative whereas drift adjustments only apply until they are overridden by a subsequent drift adjustment. Equation 2 provides a generalized calculation for the cumulative adjustment:

$$A_{t_x} = O_{t_0} + \left[O_{t_1} + D_{t_0}(t_1 - t_0)\right] + \ldots + \left[O_{t_x} + D_{t_{x-1}}(t_x - t_{x-1})\right] \quad (2)$$

Where A is the cumulative adjustment, O is adjustment for offset, D is adjustment for drift, and t is the time in years since deployment. Conditioning the DuraFET sensors in flowing seawater for a few weeks prior to deployment leads to improved sensor stability and smaller initial offsets [*Bresnahan et al.*, 2014; *Johnson et al.*, 2016], and this method has been adopted for all SOCCOM float deployments from 2016 forward. Three of the four floats analyzed here (floats 9254, 9031, and 9096) were not conditioned prior to deployment and, as a result, the adjustments that have been made to these pH sensors are larger than the current typical adjustments (see Figure S1).

While many empirical methods exist for estimating seawater TA we use estimates from a SOCCOM-specific Southern Ocean algorithm (based on T, S, P, O_2, and location; see Supporting Information for fit equation and Table S1 for fit coefficients) for this analysis. Another option for alkalinity estimation is LIAR [Locally Interpolated Alkalinity Regression; *Carter et al.*, 2016], which uses data from the GLODAP dataset [*Key et al.*, 2004] through 1999, with global resolution. The SOCCOM-specific algorithm is a more simple MLR, with one set of coefficients for the entire Southern Ocean determined using discrete bottle samples from recent (2007 to present) Southern Ocean CLIVAR and GO-SHIP repeat hydrographic cruises. LIAR and the SOCCOM-specific algorithm employ the same set of predictor variables, and TA estimates generally agree to within their standard uncertainties (6.5 and 4.7 μmol kg^{-1}, respectively). For the following analysis an average standard uncertainty in TA of 5.6 μmol kg^{-1} is used.

3. Contributions to uncertainty in calculated pCO_{2sw} (pH, TA)

To estimate the uncertainty in pCO_{2sw} estimated from pH and TA, pCO_{2sw}(pH, TA), calculated from a float-based pH measurement and an algorithm estimate of TA, we consider the contributions to uncertainty from three main components: (1) float-measured pH, (2) algorithm-estimated TA, and (3) the silicate and phosphate concentrations and carbonate system equilibrium and solubility constants used in the calculation. Figure 2 diagrams the sources of uncertainty with asterisks indicating sources that could lead to a bias in the results and plus signs indicating sources that will be considered in a separate bias assessment. Uncertainties leading to biases will be considered differently than random uncertainties because a bias leads to a larger error in calculated annual air-sea fluxes. Absolute uncertainties are expressed as values and relative uncertainties are expressed as percentages

relative to pH = 8, TA = 2300 μmol kg^{-1}, and pCO_{2sw} = 400 μatm, (e.g., absolute uncertainty of 5 μmol kg^{-1} is 0.2% relative uncertainty in TA). The word "standard" with an uncertainty estimate indicates that the value is expressed as a standard deviation with a confidence interval based on the normal distribution curve. After detailing each source of uncertainty we calculate an overall uncertainty in float pCO_{2sw} (pH, TA) using a Monte Carlo error analysis.

3.1. Float pH

For float-measured pH, there are uncertainty contributions from instrumental precision and from the calibration adjustment process. For the calculation of pCO_{2sw} (pH, TA), *Dickson and Riley* [1978] estimated that a 1% change in the hydrogen ion concentration (0.004 in pH) results in a 1.2% change in pCO_{2sw} (pH, TA); and we use this sensitivity factor to convert uncertainties in pH to uncertainties in pCO_{2sw} (pH, TA) in Table 2. The DuraFET pH sensor has a standard precision of 0.003 based on consecutive pH measurements through a well-mixed surface layer at pH ≈ 8 [*K. Johnson, unpublished data*], which converts to 0.9% relative uncertainty in pCO_{2sw} (pH, TA). During initial calibration, the responses of each DuraFET pH sensor as a function of T and P are characterized in a laboratory setting [*Johnson et al.*, 2016]. The uncertainty in the T coefficient is negligible and the uncertainty in the pressure coefficient equates to a pH uncertainty of 0.0025, resulting in 0.8% uncertainty in pCO_{2sw} (pH, TA). As shown in Figure 2, the pH sensor calibration adjustment process introduces additional uncertainty stemming from the MLR algorithm. The MLR algorithm used to adjust the pH sensor is determined using bottle measurements of pH, S, and O_2 and CTD measurements of T and P. The root mean square error (RMSE) of the MLR fit residuals in pH is 0.004 [*Williams et al.*, 2016] and the absolute uncertainty in the bottle pH measurements used to determine the algorithm is 0.0047 [*Carter et al.*, 2013]. Because the pH algorithm is determined using bottle pH data that were analyzed at lab T and P and converted to in situ conditions at 1500 m, the uncertainty introduced by this conversion must also be considered. The uncertainties in this lab-to-in-situ conversion are not well quantified but a 0.005 uncertainty is likely realistic at the ocean surface [*A. Dickson, pers. comm.*].

An additional possible source of uncertainty in pH originates from uncertainties in the float T, S, and O_2 measurements, which are required for the MLR used for pH sensor calibration adjustments. The uncertainties in the T and S data used in the application of the MLR algorithm are on the order of 0.002°C and 0.01 respectively [*Owens and Wong*, 2009]. When the algorithm is applied, the resulting pH uncertainties from the T and S terms (0.00001 and 0.0018, respectively) are several orders of magnitude smaller than the other uncertainties at hand. For Aanderaa O_2 optodes mounted on floats *Johnson et al.* [2015] found no significant drift after float deployment, whereas *Bushinsky et al.* [2015] found, on average, a 0.3% yr^{-1} drift and recommended adjusting the O_2 sensor gain correction factor over time using ongoing float-based surface air-O_2 measurements. A 0.3% yr^{-1} drift in O_2, if left uncorrected, would propagate through as a 0.4% bias in calculated pCO_{2sw} (pH, TA) over one year. Most SOCCOM floats obtain an air-O_2 measurement every 10 days, but floats that spend time under ice may not get an air-O_2 measurement for over half a year. To be conservative, we assume that floats will be recalibrated using an air O_2 measurement at minimum once per year and a 0.4% relative uncertainty contribution in pCO_{2sw} (pH, TA) from the O_2 sensor is included in this analysis.

3.2. Estimated Alkalinity

The uncertainty contribution by TA in the calculation of pCO_{2sw} (pH, TA) can be approximated by multiplying the relative uncertainty in the TA estimate, 0.24% (5.6 μmol kg^{-1} out of 2300 μmol kg^{-1}), by the $\%\partial pCO_2/\%\partial TA$ scaling factor, 1.0, given by *Dickson and*

Riley [1978]. The result is a relative uncertainty in pCO_{2sw} (pH, TA) of 0.24%, or an absolute uncertainty of 1 µatm at a pCO_{2sw} of 400 µatm. pCO_{2sw} (pH, TA) is mostly dependent on the pH and is less sensitive to TA; therefore, the choice of TA algorithm is relatively unimportant for this application. Of note is that because both LIAR and the SOCCOM-specific algorithm are primarily based on austral summer data, the uncertainties in estimated TA are likely increased when the algorithms are applied throughout the full seasonal cycle and under sea ice, where the processes affecting alkalinity are not as well understood. However, even a doubling of the uncertainty in TA in wintertime would result in just a 1-µatm increase in the absolute uncertainty in pCO_{2sw} (pH, TA), which is small compared to the other uncertainties involved in the calculation.

3.3. Carbonate system equilibrium constants and nutrient concentrations

The carbonate system solubility and equilibrium constants (K_0, K_1, and K_2), which describe the solubility of CO_2 and dissociation of the carbonate species in seawater as a function of T and S, are determined in laboratory studies and each carries its own uncertainty. Several sets of equilibrium constants are available for use in carbonate system calculations, and the choice of constants may introduce a bias in pCO_{2sw} (pH, TA) [*Wanninkhof et al.*, 1999]. Here we use the equilibrium constants of *Lueker et al.* [2000] as recommended by A. Dickson [*Wanninkhof et al.*, 2016a] because, given the choice of pH on the total scale, they provide the most consistent inter-comparison for the four measurable carbonate system parameters [*Patsavas et al.*, 2015]. The estimated uncertainty in K_0 from *Dickson and Riley* [1978] (based on *Weiss* [1974]) and estimates of the uncertainties in K_1 and K_2 are used to estimate their contributions to uncertainty in pCO_{2sw} (pH, TA). The percent change in pCO_{2sw} per percent change in each dissociation constant, K, ($\%\partial pCO_2 / \%\partial K_x$ scaling factor) given by *Dickson and Riley* [1978] is multiplied by the estimated standard relative uncertainty in K for each of the three equilibrium constants (Table S2) and the results are included in Table 2.

Concentrations for silicate and phosphate are required for carbonate system calculations because they represent another acid-base system in seawater. However, since the floats do not measure these parameters they are estimated using a subset of Southern Ocean data from the GLODAPv1 database [*Key et al.*, 2004] as a function of potential density. The difference in pCO_{2sw} (pH, TA) calculated using zero concentrations or using maximum concentrations of silicate and phosphate is around 0.6 µatm, thus they do not contribute appreciably to the bias and uncertainty.

Table 2 summarizes the sources of uncertainty described thus far.

3.4 Top-down bias assessment

Calculating pCO_{2sw} (pH, TA) from floats allows use of the data to calculate F_{CO2}, which can then be integrated over time to calculate annual net oceanic CO_2 fluxes in the Southern Ocean. After integration, the contribution to the uncertainty in estimated CO_2 uptake by random uncertainties in pCO_{2sw} (pH, TA) for any one float will decrease as the number of samples increases, while any biases (i.e. systematic uncertainties) in pCO_{2sw} (pH, TA) will remain constant and potentially lead to significant errors in F_{CO2}. Several of the uncertainties described thus far (marked with asterisks in Figure 2) are systematic. Generally, if the direction and magnitude of a bias is unknown, it should be added to the sum of the other uncertainties. However, if the direction and magnitude of a bias is known, it can be corrected, and then it is only necessary to account for the uncertainty associated with the bias correction [*CITAC and Eurachem*, 2012]. Here, the direction of each individual bias is not explicitly known. However, the following top-down assessment shows that several of these

biases (marked as "yes," accounted for in top-down bias assessment in Table 2 and with a "+" in Figure 2) partially offset one another and allows the combined overall bias to be characterized.

The equilibrium constants used in this study [*Lueker et al.*, 2000] were derived to optimize the consistency between laboratory measurements of DIC, TA, and pCO_{2sw} across a range of seawater conditions. However, this derivation did not include any direct spectrophotometric measurements for pH. As a result, there is a difference between pCO_{2sw} (pH, TA) and either directly measured pCO_{2sw} or pCO_{2sw} (DIC, TA), although the latter two roughly match each other. This difference in pCO_{2sw} (pH, TA) can be traced back to differences between pH measured spectrophotometrically and pH calculated from measured DIC and TA as described by Figure 2 of *Carter at al.* [2013]. A similar pattern was observed for the two cruises which were used to quality control the SOCCOM float pH sensor data [*Sabine et al.*, 2012; *Talley et al.*, 2015], where spectrophotometric pH is low relative to pH (DIC, TA) at lower pH and the opposite at high pH (Figure 3). This means that the SOCCOM pH data must be adjusted according to Equation 3 below prior to calculating pCO_{2sw} (pH, TA) if the result is to be consistent with direct measurements of pCO_{2sw}.

$$bias\ correction = -0.034529 \times pH(25℃) + 0.26709 \quad (3)$$

The SOCCOM floats are quality controlled at 1500 m depth where pH (25°C, 0 dbar) averages ~7.58 in the Southern Ocean. According to the empirical Equation 3 derived from the cruise bottle data the float pH values are on average 0.0054 low relative to pH (DIC, TA) at this pH, which would lead to about a 1.6% positive bias in float pCO_{2sw} (pH, TA) (6.4 µatm at pCO_{2sw} of 400 µatm) relative to a direct measurement of pCO_{2sw}. To adjust for this bias the in situ pH for each individual float profile should be adjusted according to the bias correction calculated using Equation 3 and the 1500 m pH (25°C, 0 db) value for that profile. The RMS error in the regression line shown in Figure 3 is 0.0053 and this uncertainty will be accounted for in the Monte Carlo error analysis that follows.

3.5 Monte Carlo error analysis

We use a Monte Carlo error analysis to assess the overall uncertainty due to the sources of error listed in Table 2, which accounts for the nonlinear nature of the carbonate system. The Monte Carlo error analysis involves modeling the uncertainty in calculated pCO_{2sw} (pH, TA) when the input parameters are varied randomly around their values by their respective uncertainties. The uncertainties associated with the equilibrium constants and the bottle inaccuracy in pH (marked as "yes, accounted for in top-down bias assessment" in Table 2) will not be included in the analysis, but in their place we will use the RMSE of the Figure 3 line of best fit (0.0053) as mentioned above. One thousand iterations of calculated pCO_{2sw} (pH, TA) are performed for each float profile over the full lifetimes of four SOCCOM floats (9254, 9031, 9096, and 9099). These floats span several frontal regions and represent a wide range of ocean conditions.

4. Results

After correction for known biases (marked as "yes, accounted for in top-down bias assessment" in Table 2) and running the Monte Carlo error analysis with the remaining uncertainties, the combined relative standard uncertainty of 2.4% (10 µatm at pCO_{2sw} of 400 µatm) represents the 68% confidence level of biogeochemical float-based pCO_{2sw} (pH, TA) estimates in the Southern Ocean. This work focuses on surface pCO_{2sw} estimates and does not consider the additional uncertainties that may be introduced when these calculations are

done subsurface.

To evaluate our uncertainty estimate, surface float pCO_{2sw} (pH, TA) are compared with shipboard underway pCO_{2sw} measurements [*Sutherland et al.*, 2015, 2016; *van Heuven et al.*, 2016; *Wanninkhof et al.*, 2016b] from the time and location of float deployment (Figure 4) using both the uncorrected (open circles) and the bias-corrected (solid squares) float results. The underway pCO_{2sw} data were matched by date, time, and location (±0.01° latitude and longitude) to the float deployment calibration CTD cast. The underway pCO_{2sw} data have a 1% relative uncertainty [*Takahashi et al.*, 2009] and, because pCO_{2sw} is highly temperature-dependent, the underway pCO_{2sw} data are adjusted to float T using CO2SYS [*Lewis and Wallace*, 1998; *van Heuven et al.*, 2011] in combination with float-based estimates of TA, silicate, and phosphate. The uncorrected and bias-corrected float data are both on average biased high relative to the underway data by 7.2 and 3.7 µatm, respectively. All float pCO_{2sw} data move in the same direction after bias correction because all of the floats discussed here are in regions where 1500 m pH is relatively low. The reduction in error between the two datasets indicates that the bias correction outlined in section 3.4 improves the overall agreement between the float and underway pCO_{2sw} results, and improves the accuracy of float pCO_{2sw} (pH, TA).

The remaining bias and scatter in the comparison of float and underway pCO_{2sw} could be attributed to a combination of factors. An unknown bias may be introduced to the float pH data during the quality control process as a result of the uncertainties in the effect of pressure on the carbonate system equilibrium constants, which has been measured only once [*Culberson and Pytkowicz*, 1968]. Also, the float performs its first profile after drifting at 1000 m depth for approximately 18 hours after deployment, and this time and space lag, along with the uncertainty in underway pCO_{2sw} measurements, could account for the scatter in the difference between the bias-corrected float and the underway pCO_{2sw} values. In the Southern Ocean, drifters and shipboard underway measurements have observed gradients in pCO_{2sw} that can range from 5 to 50 µatm over scales of 100 km that cannot be fully explained by gradients in SST [*Lo Monaco et al.*, 2014; *Resplandy et al.*, 2014].

5. Discussion

While float-based calculated pCO_{2sw} (pH, TA) is inherently more uncertain (2.4% relative uncertainty) than most ship- or mooring-based pCO_{2sw} measurements [*Takahashi et al.*, 2009; *Bakker et al.*, 2016] a well-calibrated array of biogeochemical floats can complement the existing global dataset by providing a seasonal context to regions where winter time measurements are sparse. Figure 5 shows the calculated ΔpCO_2 (bias-corrected pCO_{2sw} (pH, TA) – pCO_{2a} from Cape Grim) for four SOCCOM floats representing four different regions: 9254 (WMO ID 5904395) in the subtropical zone, 9031 (WMO ID 5904396) in the Subantarctic Zone (SAZ), 9096 (WMO ID 5904469) in the polar Antarctic zone, and 9099 (WMO ID 5904468) in the seasonal sea ice zone, with error bars representing 2.4% relative standard uncertainty. The pCO_{2a} values are adjusted to reflect local sea level pressure at the time of the measurement using NCEP/NCAR data available from http://www.esrl.noaa.gov/psd. Also plotted are monthly co-located ΔpCO_2 estimates from *Takahashi et al.* [2014; hereafter T14] and *Landschützer et al.* [2014, 2015; hereafter L14]. For L14, which includes monthly estimates for the years 1982−2011, an average of 2002−2011 was used to create one monthly climatology for this comparison. The RMSEs of the fits to the data from which they were trained are ±10 µatm [*Takahashi et al.*, 2009] and ±12 µatm [*Landschützer et al.*, 2014]. Positive values will cause a carbon flux out of the ocean and into the atmosphere. Time series of surface in situ float pH and algorithm TA used

to calculate pCO_{2sw} (pH, TA) for each float can be found in Figure S2.

Directly comparing pCO_{2sw} from different years requires adjusting for anthropogenic carbon uptake, which adds uncertainty, so ΔpCO_2 is used instead of pCO_{2sw} to compare the floats with climatologies. Because pCO_{2sw} is highly temperature-dependent it is also important to consider differences in sea surface temperature (SST) when comparing values for pCO_{2sw} or ΔpCO_2. A 1°C warming causes a 4.23% increase in pCO_{2sw} [*Takahashi et al.*, 1993] which at a pCO_2 near 400 µatm is ~17 µatm $°C^{-1}$. When we compare the float T with SST from the T14 climatology (Figure 6) we observe temperature differences of up to 2°C between the floats and the climatology, but only sometimes can SST differences explain the observed differences in ΔpCO_2.

Float 9254 (Figure 5a), which is located in the subtropical zone, compares reasonably well with the climatological estimates for ΔpCO_2 throughout the annual cycle with the exception that the float observes a few anomalously high ΔpCO_2 values in the summers of 2015 and 2016. A comparison of float 9254 and T14 climatological SST (Figure 6a) reveals that the area where the float surfaced was anomalously warm at those times, and this could explain the summertime differences in ΔpCO_2. However, there were other times when float 9254 was warmer than the climatological SST but the float did not observe significantly different ΔpCO_2 from the climatologies.

For float 9031 (Figure 5b), which is just north of the Subantarctic Front of the Antarctic Circumpolar Current (ACC) in the Pacific sector of the SAZ, calculated ΔpCO_{2sw} matches well with climatological estimates that show the region to be a weak sink for CO_2 throughout the year. The SST observed by the float matches well with the climatological SST (Figure 6b).

In contrast, there is significant disagreement between the climatologies and float 9096, which is located south of the ACC in the Atlantic sector of the polar Antarctic Zone (Figure 5c). Both climatological estimates imply a nearly neutral oceanic sink/source for CO_2 while the float-calculated ΔpCO_2 is mostly positive, implying that the region occupied by this float was a strong CO_2 source for around two-thirds of the year each year. Float 9096 is consistently cooler than the climatological SST (Figure 6c) and this temperature difference alone would cause the float ΔpCO_2 to be lower than the climatological ΔpCO_2, but we observe the opposite. The large differences in ΔpCO_2 between the float and the climatologies occur in winter months when upwelling and entrainment are dominant drivers of surface ocean pCO_{2sw}. An increase in the strength of the upwelling or an increase in the DIC of the upwelled waters could explain this observed increase in ΔpCO_2. *Williams et al.* [2015] observed an increase in the DIC of circumpolar deep waters (the source of upwelled waters in this region) of around 12 µmol kg^{-1} in the Pacific sector of the Southern Ocean between 1992 and 2011; *Woosley et al.* [2016] and *Wanninkhof et al.* [2010] found similar increases in the Atlantic sector over a similar time period.

Float 9099 (Figure 5d), located in the seasonal sea ice zone in the Atlantic sector and covered by sea ice between May and November, is in better agreement with L14 in both the magnitude of the seasonal cycle and time-evolution of ΔpCO_2 than with the T14 climatology. As with float 9096, the SST observed by the float is lower on average than the climatological T14 SST and explains the summertime but not the wintertime differences in ΔpCO_2. *Takahashi et al.* [2009], used underway data from six north-south wintertime transects to estimate pCO_{2sw} for regions with partial ice coverage as a function of the day of the year and

then used this relationship to represent the pCO_{2sw} in the entirety of the climatological Antarctic seasonal sea ice zone. The *Takahashi et al.* [2009] relationship ($pCO_{2sw} = 0.802 \times$ day of year + 208.9) along the float 9099 track results in T14 ΔpCO_2 increasing through time until September, and then declining, whereas the float ΔpCO_{2sw} stays positive until October or November, when the ice begins to break up and outgassing and biological drawdown of CO_2 brings ΔpCO_2 back toward negative values.

In general, the climatologies tend to agree with the floats within their respective uncertainties during the austral summer when there are significantly more underway pCO_{2sw} data to create the climatology. Large disagreements arise when there are no suitable data to constrain the climatology, such as austral winter and in ice-covered waters. This disagreement is not surprising, considering (1) the limited availability of austral winter and under-ice observations to compute the climatologies, and (2) the pCO_{2sw} climatologies are based on climatological sea ice cover, which may differ from float observations. L14 attempt to overcome data limitations through the use of a self-organizing map to cluster available pCO_{2sw} data into geochemical provinces, using T, S, mixed layer depth, and climatological pCO_{2sw} from *Takahashi et al.* [2009]. These geochemical provinces are allowed to evolve with time, and data from the Southern Ocean seasonal sea ice zone are often combined with data from other similar ocean regions to estimate the L14 pCO_{2sw} climatology. However, the disagreements with the float data are similar to that of T14 because the geochemical provinces are constructed, in part, using the same pCO_{2sw} data and suffer from wintertime data limitation.

While the calculation of the magnitude of the CO_2 flux relies on several other factors such as wind speed and solubility, which each bring significant additional uncertainties, the direction of the flux at a given time is determined by the sign of ΔpCO_2. In addition to illuminating the source or sink component of the CO_2 flux in these frontal regions, the float pCO_{2sw} (pH, TA) estimates reveal that the magnitude of the seasonal cycles in pCO_{2sw} in the subtropical zone, polar Antarctic zone, and seasonal sea ice zone are larger than estimated by currently-available climatologies. These biogeochemical floats will also be useful in constraining processes controlling gas flux in partial sea ice coverage because of their capability to sample under sea ice, and because the errors in TA estimation are less important than other errors in the pCO_{2sw} (pH, TA) calculation. Because these floats have a lifetime of up to five years they can also provide insights into interannual variability in pCO_{2sw} and F_{CO2} and their drivers as well as provide contrast between various oceanographic regimes as they migrate across fronts and in and out of eddies. An array of floats providing data on 10-day timescales has a strong potential to significantly improve our understanding of the effect that large-scale climate variability has on the air-sea CO_2 flux in the Southern Ocean [*Majkut et al.*, 2014].

6. Conclusions

Ongoing shipboard and moored observation programs show that the pCO_{2sw} is increasing globally as a result of anthropogenic emissions. Nonetheless, our current understanding of the seasonal cycle and interannual variability, and thus the mechanisms controlling pCO_{2sw} and air-sea CO_2 flux, is lacking over many parts of the world ocean. Despite the estimated 2.4% relative standard uncertainty in current biogeochemical float-based pCO_{2sw} (pH, TA) estimates, it is clear from the differences between existing climatologies and new float pH-based pCO_{2sw} (pH, TA) estimates that incorporating information from these novel carbon observational platforms can improve climatologies, climate models, and future projections. While true space/time crossovers between biogeochemical floats and shipboard pCO_2 systems are rare, and spatial and temporal heterogeneity make direct comparisons difficult,

we have shown that a well-calibrated biogeochemical float provides meaningful data that strengthen the current body of pCO_{2sw} observations.

Maintaining a well-calibrated biogeochemical float array for estimating carbonate system parameters relies on high-quality shipboard measurements of pH and oxygen to anchor the sensor data at deployment and float-based air oxygen measurements to adjust the float calibration beyond the initial deployment cast. While early SOCCOM floats exhibited pH sensor drift and relied heavily upon the MLR algorithms for calibration adjustments, the pH sensors deployed during the 2015/2016 field season equilibrated with natural seawater prior to deployment [*Bresnahan et al.*, 2014; *Johnson et al.*, 2016] show no sign of significant drift to date as compared with the empirical algorithms. As float-based sensors continue to improve, the uncertainties in float-based pCO_{2sw} (pH, TA) estimates should decrease. However, the uncertainty in calculated pCO_{2sw} (pH, TA) resulting from uncertainties in the carbonate system equilibrium and solubility constants will likely remain. Due to the significant value added, well-calibrated float pH-based pCO_{2sw} (pH, TA) along with other derived variables, such as aragonite and calcite saturation state, should be included in future data-compiling efforts and climatological estimates while taking into account the estimated uncertainty in these calculated quantities. We believe that this uncertainty analysis will aid in the consideration and planning for a future global biogeochemical array [*Johnson and Claustre*, 2016].

Acknowledgments
All SOCCOM float and calibration cruise data used in this study are available at http://www3.mbari.org/soccom/SOCCOM_Data_Archive. Other discrete and underway cruise data used in this study are available at https://cchdo.ucsd.edu. This work was sponsored by the U.S. National Science Foundation's Southern Ocean Carbon and Climate Observations and Modeling (SOCCOM) Project under the NSF Award PLR-1425989, supplemented by NASA (NNX14AP49G). Additionally, we acknowledge support from U.S. Argo through NOAA/JISAO grant NA17RJ1232 to the University of Washington. Logistical support for this project in Antarctic waters was provided by the U.S. National Science Foundation through the U.S. Antarctic Program and the U.S. GO-SHIP program, Australia's CSIRO, and Germany's Alfred Wegener Institute. Richard Feely was supported by the Ocean Observations and Monitoring Division, Climate Program Office, National Oceanic and Atmospheric Administration, U.S. Department of Commerce. Work done at Monterey Bay Aquarium Research Institute was supported by the David and Lucile Packard Foundation. Alison Gray was supported by a NOAA Climate and Global Change postdoctoral fellowship. Nancy Williams is also supported by the ARCS Foundation Oregon Chapter. We would like to thank A. Fassbender and B. Carter for helpful discussions, and we gratefully acknowledge Are Olsen and an anonymous reviewer for insightful comments that have strengthened this manuscript. This is PMEL contribution number 4547.

References

Bakker, D. C. E. et al. (2016), A multi-decade record of high-quality fCO_2 data in version 3 of the Surface Ocean CO_2 Atlas (SOCAT), *Earth Syst. Sci. Data*, doi:10.5194/essd-2016-15.

Bresnahan, P. J., T. R. Martz, Y. Takeshita, K. S. Johnson, and M. LaShomb (2014), Best practices for autonomous measurement of seawater pH with the Honeywell Durafet, *Methods Oceanogr.*, *9*, 44–60, doi:10.1016/j.mio.2014.08.003.

Bushinsky, S. M., S. R. Emerson, S. C. Riser, and D. D. Swift (2016), Accurate oxygen measurements on modified Argo floats using in situ air calibrations, *Limnol. Oceanogr. Methods*, *14*(8), 491–505, doi:10.1002/lom3.10107.

Carter, B. R., J. A. Radich, H. L. Doyle, and A. G. Dickson (2013), An automated system for spectrophotometric seawater pH measurements, *Limnol. Oceanogr. Methods*, *11*, 16–27, doi:10.4319/lom.2013.11.16.

Carter, B. R., N. L. Williams, A. R. Gray, and R. A. Feely (2016), Locally interpolated alkalinity regression for global alkalinity estimation, *Limnol. Oceanogr. Methods*, *14*(4), 268–277, doi:10.1002/lom3.10087.

CITAC, and Eurachem (2012), *Quantifying Uncertainty in Analytical Measurement*, 3rd ed., edited by S. L. R. Ellison and A. Williams.

Culberson, C., and R. M. Pytkowicz (1968), Effect of Pressure on Carbonic Acid, Boric Acid and the pH in Seawater, *Limnol. Oceanogr.*, *13*(3), 403–417.

Dickson, A. G. (1990), Standard potential of the reaction: $AgCl(s) + 1/2\ H_2(g) = Ag(s) + HCl(aq)$, and the standard acidity constant of the ion HSO_4^- in synthetic sea water from 273.15 to 318.15 K, *J. Chem. Thermodyn.*, *22*(2), 113–127, doi:10.1016/0021-9614(90)90074-Z.

Dickson, A. G., and J. P. Riley (1978), The effect of analytical error on the evaluation of the components of the aquatic carbon-dioxide system, *Mar. Chem.*, *6*(1), 77–85, doi:10.1016/0304-4203(78)90008-7.

Frölicher, T. L., J. L. Sarmiento, D. J. Paynter, J. P. Dunne, J. P. Krasting, and M. Winton (2015), Dominance of the Southern Ocean in Anthropogenic Carbon and Heat Uptake in CMIP5 Models, *J. Clim.*, *28*(2), 862–886, doi:10.1175/JCLI-D-14-00117.1.

van Heuven, S., D. Pierrot, J. W. B. Rae, E. Lewis, and D. W. R. Wallace (2011), *MATLAB Program Developed for CO_2 System Calculations. ORNL/CDIAC-105b*, Carbon Dioxide Information Analysis Center, Oak Ridge National Laboratory, U.S. Department of Energy, Oak Ridge, Tennessee.

van Heuven, S., M. Hoppema, and O. Boebel (2016), *Surface measurements of pCO_2 data obtained during the SOCCOM float deployment expedition onboard R/V Polarstern cruise ANTXXX_2 (2 December 2014 – 1 February 2015)*, Carbon Dioxide Information Analysis Center, Oak Ridge National Laboratory, US Department of Energy, Oak Ridge, Tennessee.

Johnson, K. S., and H. Claustre (2016), Bringing Biogeochemistry into the Argo Age, *Eos (Washington. DC).*, (97), doi:10.1029/2016EO062427.

Johnson, K. S., J. N. Plant, S. C. Riser, and D. Gilbert (2015), Air oxygen calibration of oxygen optodes on a profiling float array, *J. Atmos. Ocean. Technol.*, *32*(11), 2160–2172, doi:10.1175/JTECH-D-15-0101.1.

Johnson, K. S., H. W. Jannasch, L. J. Coletti, V. A. Elrod, T. R. Martz, Y. Takeshita, R. J. Carlson, and J. G. Connery (2016), Deep-Sea DuraFET: A Pressure Tolerant pH Sensor Designed for Global Sensor Networks, *Anal. Chem.*, *88*(6), 3249–3256, doi:10.1021/acs.analchem.5b04653.

Key, R. M., A. Kozyr, C. L. Sabine, K. Lee, R. Wanninkhof, J. L. Bullister, R. A. Feely, F. J. Millero, C. Mordy, and T. H. Peng (2004), A global ocean carbon climatology: Results

from Global Data Analysis Project (GLODAP), *Global Biogeochem. Cycles*, *18*(4), doi:10.1029/2004GB002247.

Landschützer, P., N. Gruber, D. C. E. Bakker, and U. Schuster (2014), Recent variability of the global ocean carbon sink, *Global Biogeochem. Cycles*, *28*(9), 927–949, doi:10.1002/2014GB004853.

Landschützer, P., N. Gruber, and D. C. E. Bakker (2015), An observation-based global monthly gridded sea surface pCO_2 product from 1998 through 2011 and its monthly climatology, *Global Biogeochem. Cycles*, doi:10.3334/CDIAC/OTG.SPCO2_1982_2011_ETH_SOM-FFN.

Lee, K., T.-W. Kim, R. H. Byrne, F. J. Millero, R. A. Feely, and Y.-M. Liu (2010), The universal ratio of boron to chlorinity for the North Pacific and North Atlantic oceans, *Geochim. Cosmochim. Acta*, *74*(6), 1801–1811, doi:10.1016/j.gca.2009.12.027.

Lewis, E., and D. W. R. Wallace (1998), *Program Developed for CO_2 System Calculations*, Carbon Dioxide Information Analysis Center, Oak Ridge National Laboratory, U.S. Department of Energy, Oak Ridge, Tennessee.

Lueker, T. J., A. G. Dickson, and C. D. Keeling (2000), Ocean pCO_2 calculated from dissolved inorganic carbon, alkalinity, and equations for K_1 and K_2: validation based on laboratory measurements of CO_2 in gas and seawater at equilibrium, *Mar. Chem.*, *70*(1–3), 105–119, doi:10.1016/S0304-4203(00)00022-0.

Majkut, J. D., B. R. Carter, T. L. Frolicher, C. O. Dufour, K. B. Rodgers, and J. L. Sarmiento (2014), An observing system simulation for Southern Ocean carbon dioxide uptake, *Philos. Trans. R. Soc. A Math. Phys. Eng. Sci.*, *372*(2019), 20130046, doi:10.1098/rsta.2013.0046.

Lo Monaco, C., N. Metzl, F. D'Ovidio, J. Llort, and C. Ridame (2014), Rapid establishment of the CO_2 sink associated with Kerguelen's bloom observed during the KEOPS2/OISO20 cruise, *Biogeosciences Discuss.*, *11*(12), 17543–17578, doi:10.5194/bgd-11-17543-2014.

Owens, W. B., and A. P. S. Wong (2009), An improved calibration method for the drift of the conductivity sensor on autonomous CTD profiling floats by θ–S climatology, *Deep Sea Res. Part I Oceanogr. Res. Pap.*, *56*(3), 450–457, doi:10.1016/j.dsr.2008.09.008.

Patsavas, M. C., R. H. Byrne, R. Wanninkhof, R. A. Feely, and W.-J. Cai (2015), Internal consistency of marine carbonate system measurements and assessments of aragonite saturation state: Insights from two U.S. coastal cruises, *Mar. Chem.*, *176*, 9–20, doi:10.1016/j.marchem.2015.06.022.

Perez, F. F., and F. Fraga (1987), Association constant of fluoride and hydrogen ions in seawater, *Mar. Chem.*, *21*(2), 161–168, doi:10.1016/0304-4203(87)90036-3.

Le Quéré, C. et al. (2016), Global Carbon Budget 2016, *Earth Syst. Sci. Data Discuss.*, 1–3, doi:10.5194/essd-2016-51.

Resplandy, L., J. Boutin, and L. Merlivat (2014), Observed small spatial scale and seasonal variability of the CO_2 system in the Southern Ocean, *Biogeosciences*, *11*(1), 75–90, doi:10.5194/bg-11-75-2014.

Sabine, C. L., R. A. Feely, R. Wanninkhof, A. G. Dickson, F. J. Millero, D. A. Hansell, and J. H. Swift (2012), *Carbon Dioxide, Hydrographic, and Chemical Data Obtained During the R/V* Nathaniel B. Palmer *Cruise in the Southern Ocean on CLIVAR Repeat Hydrography Section S04P (Feb. 19 - Apr. 23, 2011)*, Oak Ridge, Tennessee.

Sutherland, S. C., T. Newberger, T. Takahashi, and C. Sweeney (2015), *Report of underway pCO_2 measurements in surface waters and the atmosphere during March - May 2014 R/V Nathaniel B. Palmer Cruise 14/3*, Lamont-Doherty Earth Observatory of Columbia University, Palisades, NY 10964.

Sutherland, S. C., T. Newberger, T. Takahashi, and C. Sweeney (2016), *Report of underway*

pCO_2 measurements in surface waters and the atmosphere during December 2015 R/V Nathaniel B. Palmer Cruise 15/11, Lamont-Doherty Earth Observatory of Columbia University, Palisades, NY 10964.

Takahashi, T., J. Olafsson, J. G. Goddard, D. W. Chipman, and S. C. Sutherland (1993), Seasonal variation of CO_2 and nutrients in the high-latitude surface oceans: A comparative study, *Global Biogeochem. Cycles*, *7*(4), 843–878, doi:10.1029/93GB02263.

Takahashi, T. et al. (2009), Climatological mean and decadal change in surface ocean pCO_2, and net sea–air CO_2 flux over the global oceans, *Deep. Res. II*, *56*(8–10), 554–577, doi:10.1016/j.dsr2.2008.12.009.

Takahashi, T., S. C. Sutherland, D. W. Chipman, J. G. Goddard, and C. Ho (2014), Climatological distributions of pH, pCO_2, total CO_2, alkalinity, and $CaCO_3$ saturation in the global surface ocean, and temporal changes at selected locations, *Mar. Chem.*, *164*, 95–125, doi:10.1016/j.marchem.2014.06.004.

Takahashi, T., S. C. Sutherland, and A. Kozyr (2016), *Global Ocean Surface Water Partial Pressure of CO_2 Database: Measurements Performed During 1957-2015 (Version 2015). ORNL/CDIAC-160, NDP-088(V2015)*, Carbon Dioxide Information Analysis Center, Oak Ridge National Laboratory, U.S. Department of Energy, Oak Ridge, Tennessee.

Talley, L. D., R. A. Feely, A. G. Dickson, J. H. Swift, C. A. Carlson, M. Warner, A. P. McNichol, R. M. Key, and P. Schlosser (2015), *Carbon Dioxide, Hydrographic, and Chemical Data Obtained During the RVIB Nathaniel B. Palmer Repeat Hydrography Cruises in the Pacific Ocean: GO-SHIP Sections P16S_2014 (20 March - 5 May, 2014)*, Carbon Dioxide Information Analysis Center, Oak Ridge National Laboratory, US Department of Energy, Oak Ridge, Tennessee.

Wanninkhof, R., E. Lewis, R. A. Feely, and F. J. Millero (1999), The optimal carbonate dissociation constants for determining surface water pCO_2 from alkalinity and total inorganic carbon, *Mar. Chem.*, *65*(3–4), 291–301, doi:10.1016/S0304-4203(99)00021-3.

Wanninkhof, R., S. C. Doney, J. L. Bullister, N. M. Levine, M. Warner, and N. Gruber (2010), Detecting anthropogenic CO_2 changes in the interior Atlantic Ocean between 1989 and 2005, *J. Geophys. Res.*, *115*, C11028, doi:10.1029/2010JC006251.

Wanninkhof, R. et al. (2016a), *An evaluation of pH and NO3 sensor data from SOCCOM floats and their utilization to develop ocean inorganic carbon products: A summary of discussions and recommendations of the Carbon Working Group (CWG) of SOCCOM*, Princeton Environmental Institute, Princeton, New Jersey.

Wanninkhof, R., K. Sullivan, and D. Pierrot (2016b), *Underway pCO_2 Measurements in Surface Waters and the Atmosphere During the R/V Roger Revelle GO-SHIP cruise along the section I08S_2016 (February 8 - March 15, 2016)*, Carbon Dioxide Information Analysis Center, Oak Ridge National Laboratory, US Department of Energy, Oak Ridge, Tennessee.

Weiss, R. F. (1974), Carbon dioxide in water and seawater: the solubility of a non-ideal gas, *Mar. Chem.*, *2*(3), 203–215, doi:10.1016/0304-4203(74)90015-2.

Williams, N. L., R. A. Feely, C. L. Sabine, A. G. Dickson, J. H. Swift, L. D. Talley, and J. L. Russell (2015), Quantifying Anthropogenic Carbon Inventory Changes in the Pacific Sector of the Southern Ocean, *Mar. Chem.*, *174*, 147–160, doi:10.1016/j.marchem.2015.06.015.

Williams, N. L., L. W. Juranek, K. S. Johnson, R. A. Feely, S. C. Riser, L. D. Talley, J. L. Russell, J. L. Sarmiento, and R. Wanninkhof (2016), Empirical algorithms to estimate water column pH in the Southern Ocean, *Geophys. Res. Lett.*, *43*(7), 3415–3422, doi:10.1002/2016GL068539.

Woosley, R. J., F. J. Millero, and R. Wanninkhof (2016), Rapid anthropogenic changes in CO_2 and pH in the Atlantic Ocean: 2003-2014, *Global Biogeochem. Cycles*, *30*(1), 70–90, doi:10.1002/2015GB005248.

Tables and their captions:

Table 1. Float pH sensor quality control adjustment record

SOCCOM float ID	deployment calibration CTD station	~days since deployment	adjustment for offset[1]	adjustment for drift[2] (yr^{-1})	cumulative adjustment[1]
9254	station 53 of P16S 2014 GO-SHIP cruise; 20 April, 2014	0	-0.0217	0	-0.0217
		6	0.029	0.125	0.0073
		43	0.002	-0.028	0.0220
		291	0	0	0.0030
9031	station 27 of P16S 2014 GO-SHIP cruise; 11 April, 2014	0	-0.0237	0	-0.0237
		5	-0.033	0	-0.0567
		11	0.013	-0.135	-0.0437
		187	0	-0.036	-0.1088
		339	-0.004	-0.005	-0.1277
		582	0	0	-0.1311
9096	station 12 of A12/PS89; 10 Dec, 2014	0	-0.2770	0	-0.2770
		10	0.0500	0	-0.2270
		70	-0.0130	-0.059	-0.2400
		190	-0.002	-0.078	-0.2614
		390	0.002	-0.036	-0.3021
		670	0	0	-0.3297
9099 [3]	station 78 of A12/PS89; 19 Jan, 2015	0	-0.0097	0	-0.0097
		170	0.0000	0	-0.0097
		240	-0.0130	0.017	-0.0227
		350	-0.002	-0.005	-0.0196
		500	0.003	0	-0.0186
		640	-0.0090	0	-0.0276

[1]Offset is negative when sensor pH is low compared to MLR pH estimate
[2]Drift rate is negative when sensor pH is drifting lower
[3]Float 9099 was conditioned in flowing seawater before deployment

Table 1. Float pH sensor quality control adjustment record

Table 2. Summary of uncertainties in pCO_{2sw}

	standard uncertainty in parameter	resulting relative uncertainty in pCO_{2sw}	absolute uncertainty at pCO_{2sw} = 400 µatm (µatm)	accounted for in top-down bias assessment?
pH sensor precision	0.0030	0.9%	3.6	
uncertainty in pH sensor resulting from uncertainty in pressure coefficient	0.0025	0.8%	3.0	
RMS error of MLR pH introduced through calibration	0.0040	1.2%	4.8	
bottle pH inaccuracy[a] introduced through calibration	0.0047	1.4%	5.6	yes
lab to in situ pH conversion uncertainty introduced through calibration	0.0050	1.5%	6.0	
uncertainty in float O_2 sensor measurements introduced through calibration	0.3%	0.4%	1.6	
uncertainty in float S sensor measurements introduced through calibration	0.01	0.5%	1.8	
uncertainty in float T sensor measurements introduced through calibration	0.002	0.003%	0.01	
uncertainty in estimated Alkalinity	5.6 µmol kg^{-1}	0.24%	1.0	
% uncertainty in K_0[b]	0.50	0.50%	2.0	yes
% uncertainty in K_1	1.73	1.71%	6.8	yes
% uncertainty in K_2	3.45	0.72%	2.9	yes

[a] from *Carter et al.* [2013]
[b] from *Dickson and Riley* [1978]

Table 2. Summary of uncertainties in pCO_{2sw}

Figure captions:

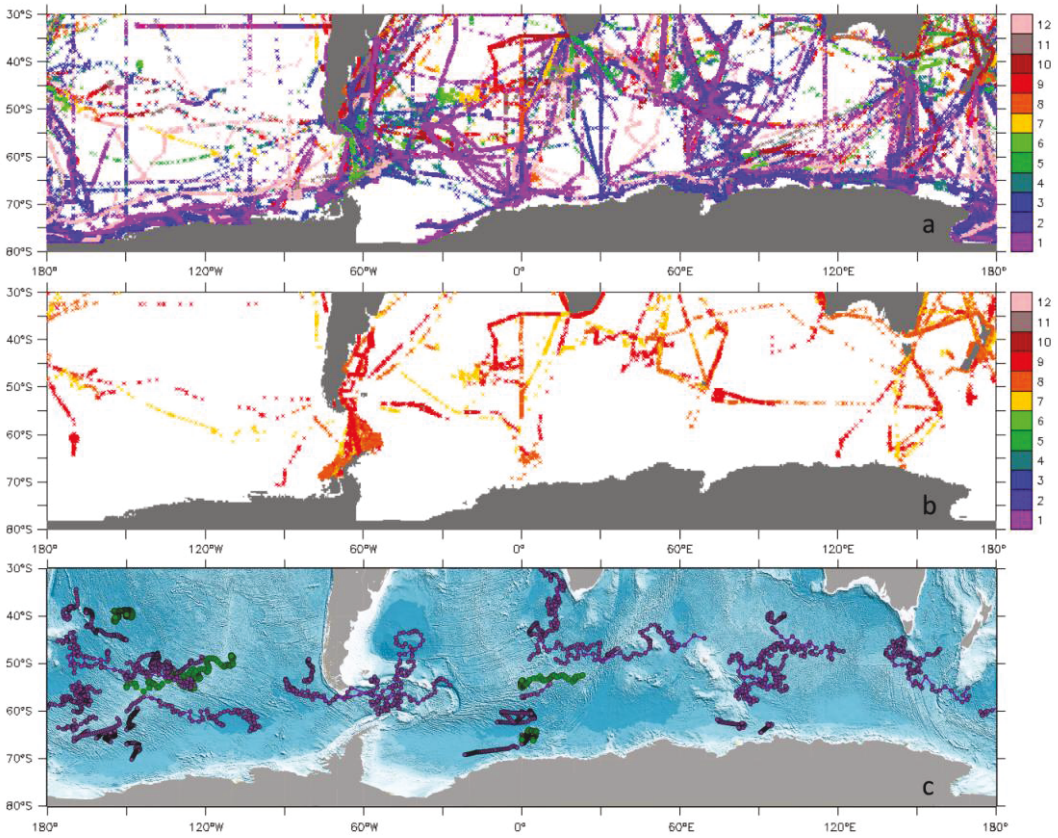

Figure 1. SOCATv4 pCO_{2sw} data [*Bakker et al.*, 2016] south of 30°S colored by month for years 1957−2015 for all months (a) and for only austral winter months (July−September; b). A map of trajectories of all SOCCOM floats from 26 March, 2014 to 4 January, 2017 with the floats used in this study colored in green (c).

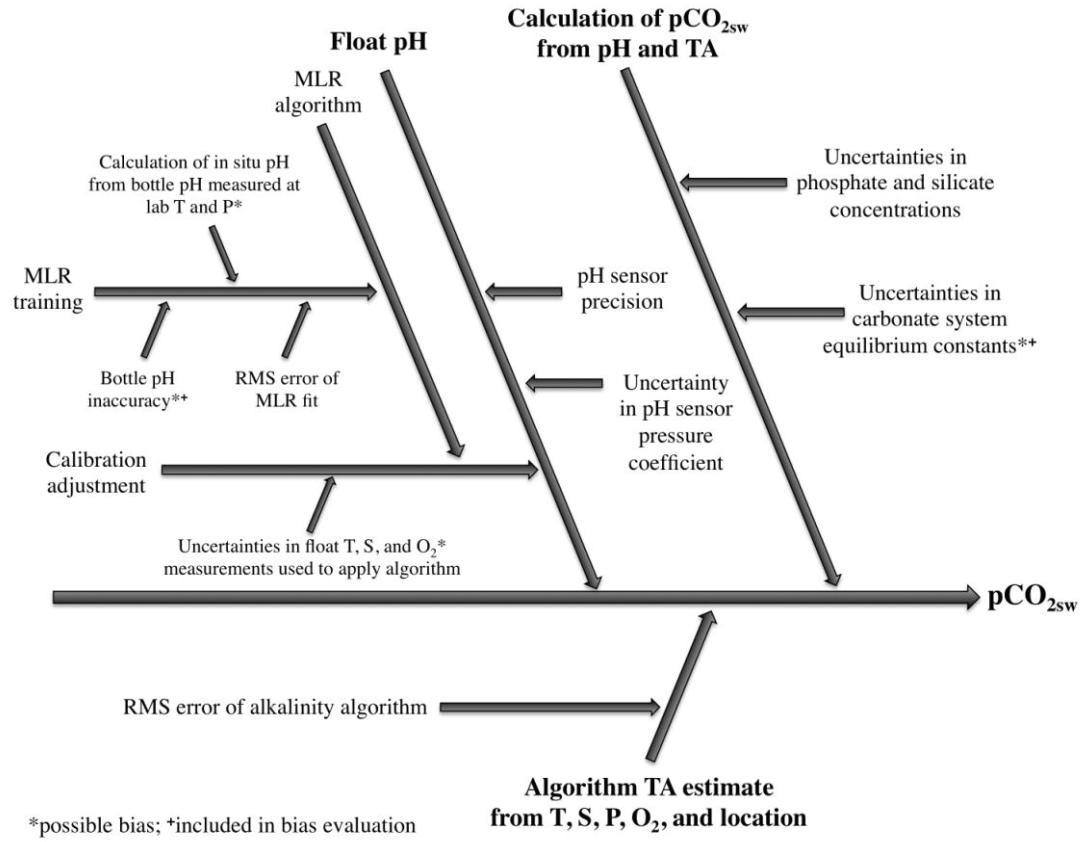

Figure 2. Diagram of contributions to the uncertainty in float-calculated pCO_{2sw} (pH, TA) using float pH and an algorithm TA estimate.

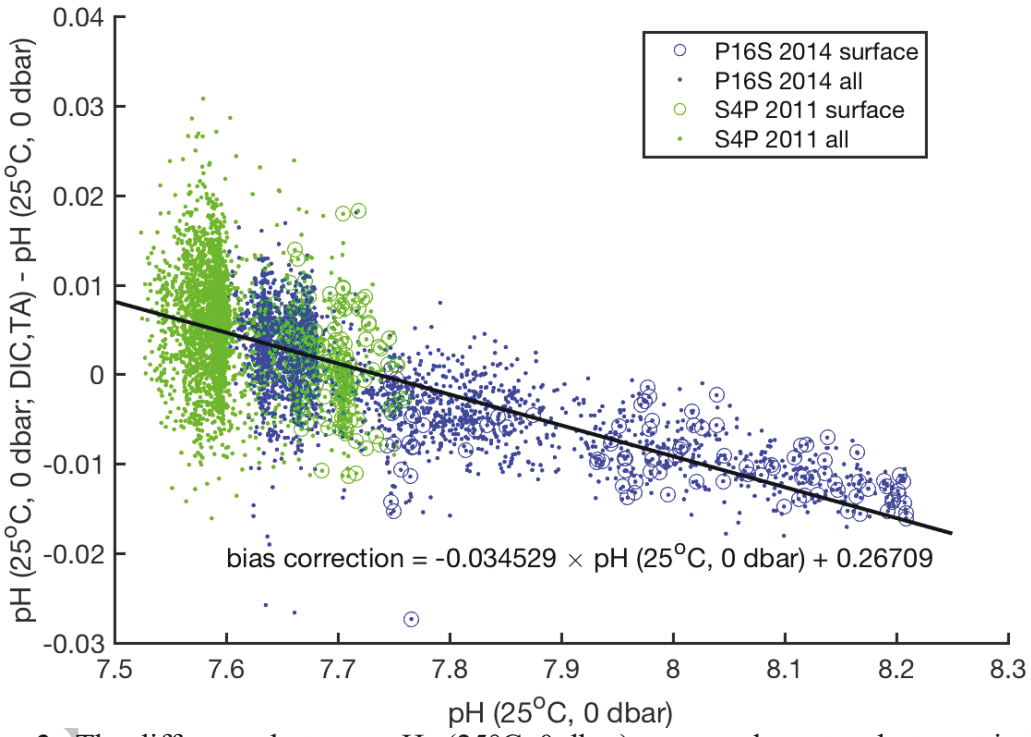

Figure 3. The difference between pH_T (25°C, 0 dbar) measured spectrophotometrically and pH_T (DIC, TA) plotted as a function of pH_T (25°C, 0 dbar) for the two GO-SHIP/SOCCOM deployment cruises used to quality control the float pH sensor data.

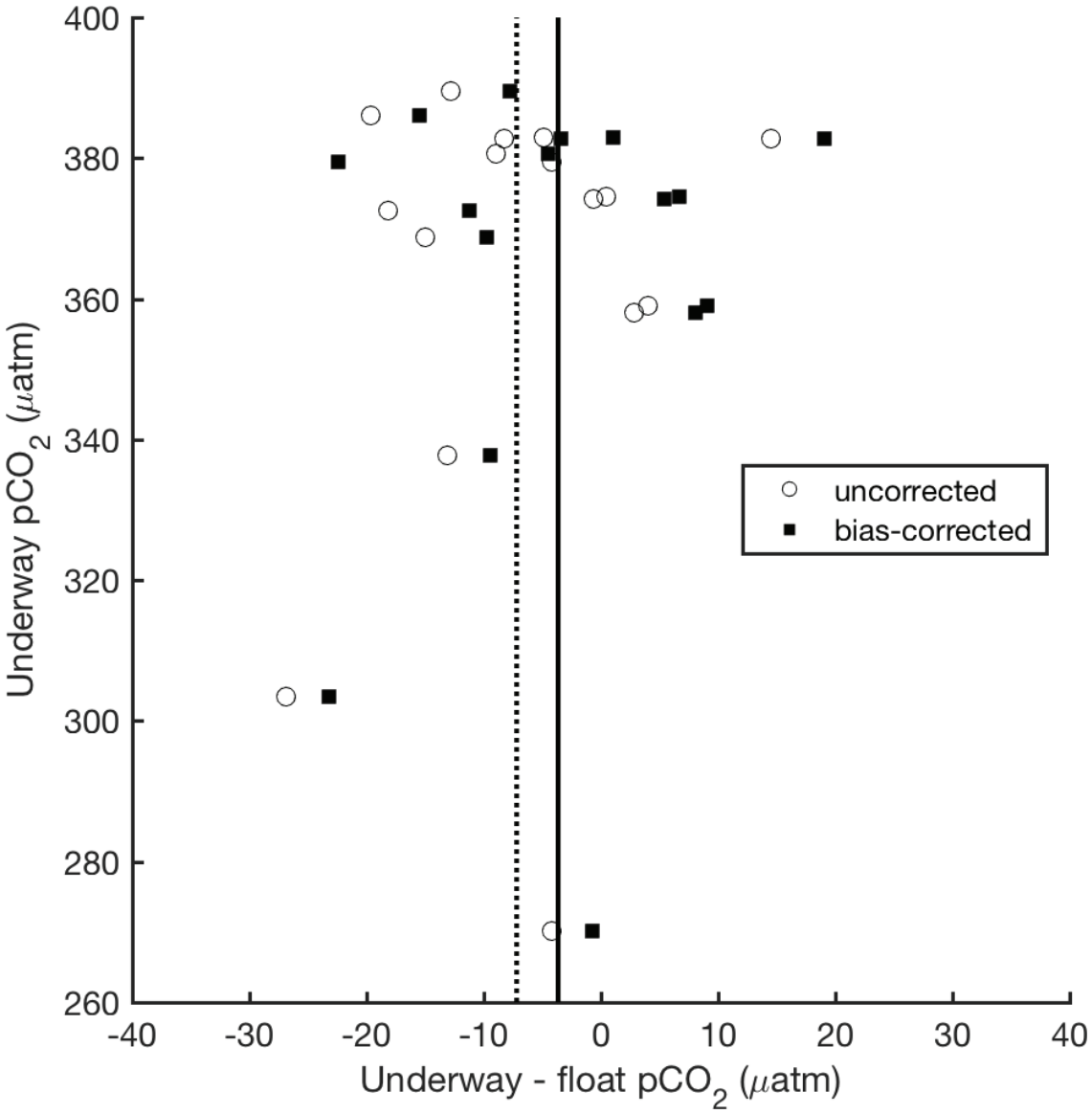

Figure 4. The difference between surface float pCO_{2sw} (pH, TA) from the first float profile and shipboard underway pCO_{2sw} [*Sutherland et al.*, 2015; *Takahashi et al.*, 2016; *van Heuven et al.*, 2016; *Wanninkhof et al.*, 2016b] at the time and location of the float deployment and calibration CTD cast for 16 SOCCOM floats. Open circles represent the uncorrected float data and solid squares represent the bias-corrected float data. The average differences for the uncorrected and bias-corrected float data are shown in the dotted and solid lines, respectively.

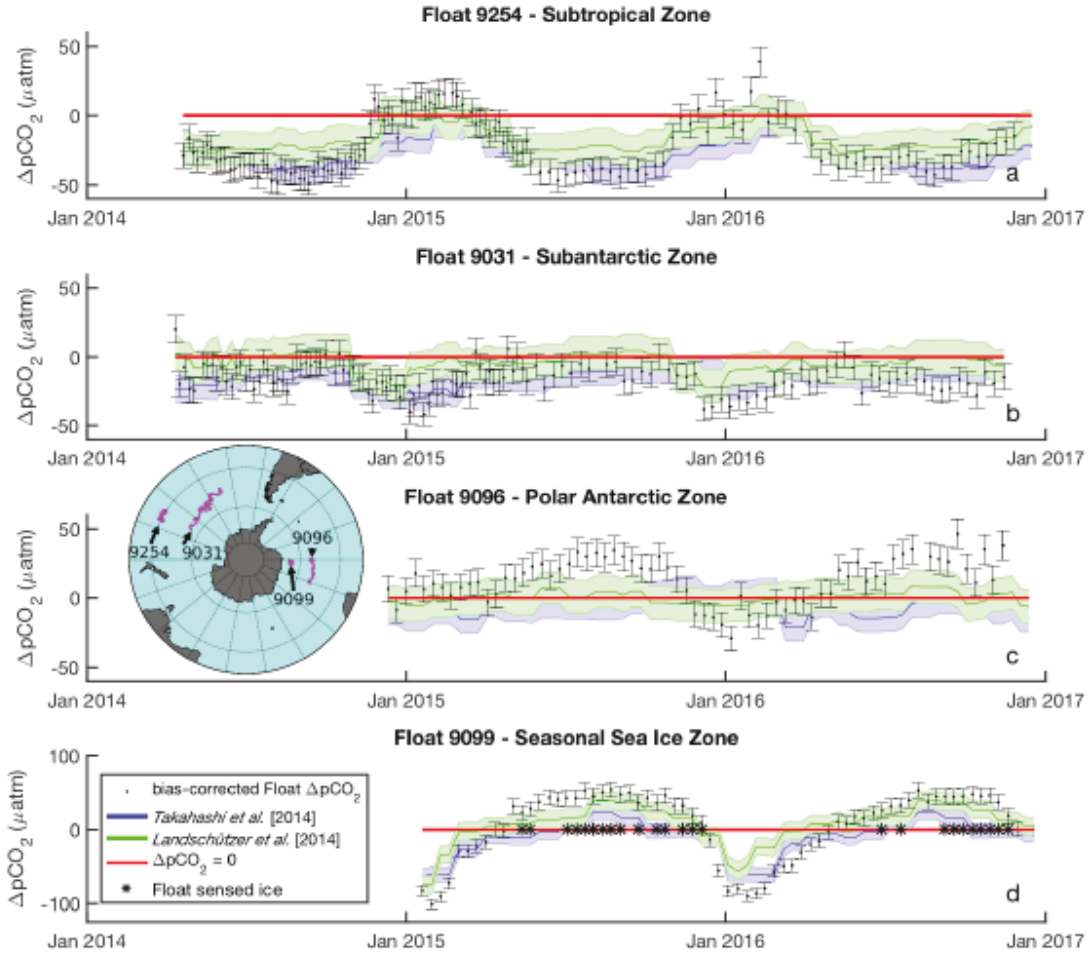

Figure 5. Bias-corrected calculated ΔpCO_{2sw} for SOCCOM floats 9254 (a), 9031 (b), 9096 (c), and 9099 (d) with error bars representing 2.4% relative uncertainty and nearby climatological estimates from *Takahashi et al.* [2014] and the *Landschützer et al.* [2014, 2015] data product (averaged over the years 2002−2011). Positive values indicate carbon flux out of the ocean and into the atmosphere. Inset map shows float locations as of 21 December, 2016.

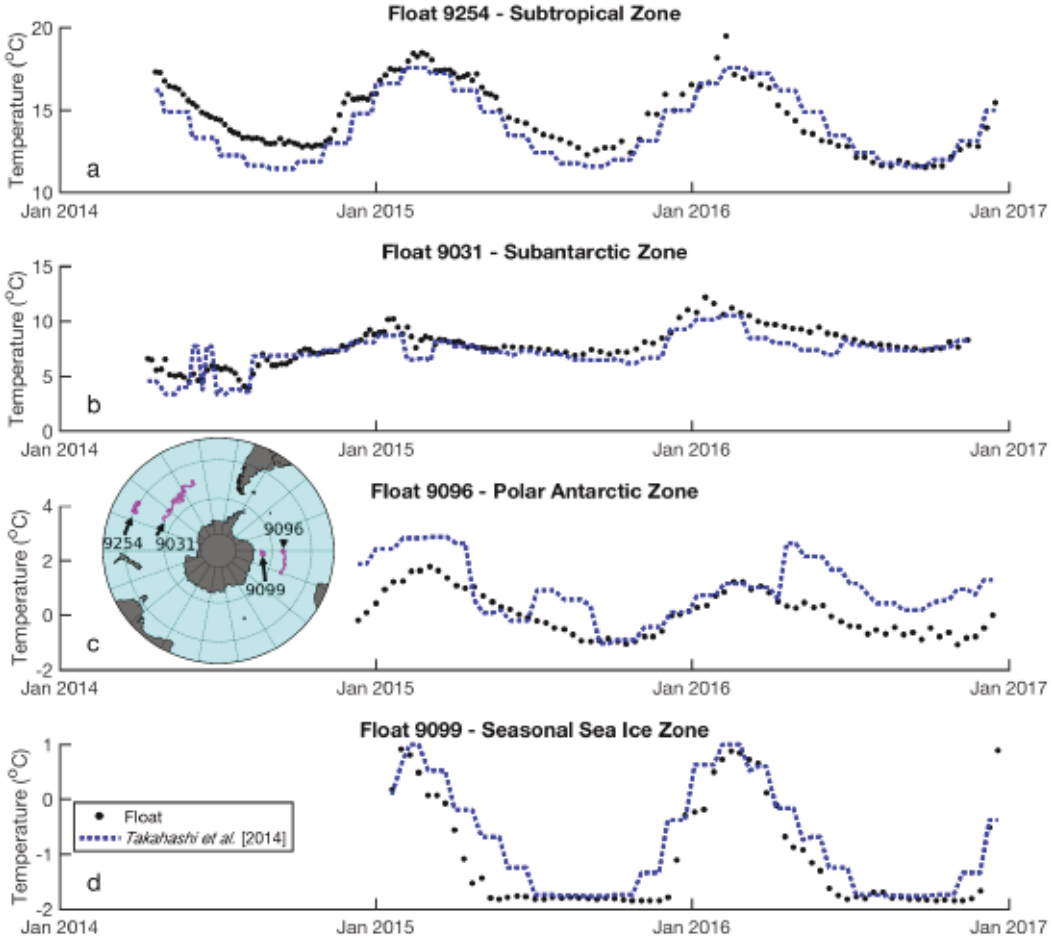

Figure 6. The sea surface temperature measured by the float (black dots) compared with co-located climatological sea surface temperature from *Takahashi et al.* [2014; blue dashed line]. Inset map shows float locations as of 21 December, 2016.